ELSEVIER

Chemical Physics 267 (2001) 81–92

Chemical Physics

www.elsevier.nl/locate/chemphys

Coherent control of atom–diatom reactive scattering: isotopic variants of $H + H_2$ in three dimensions

Alexander Abrashkevich, Moshe Shapiro [1], Paul Brumer *

Chemical Physics Theory Group, University of Toronto, Photonics Research Ontario, Toronto, Canada M5S 3H6

Received 3 January 2001

Abstract

Control over reactive and non-reactive cross-sections in 3D atom–diatom scattering is shown to be possible using a superposition of non-degenerate ro-vibrational states of the target-diatomic molecule. Depending on the phase and magnitude of the coefficients which describe the initial superposition state, one can, through quantum interference, enhance or suppress the reactive or non-reactive scattering to predetermined product states. Fully converged 3D quantum computations reveal extensive control over the reactive/non-reactive branching ratios in the $D + H_2 \rightarrow DH + H$ and the $H + H'D \rightarrow HH' + D$; $HD + H'$ reactions, where H and H′ denote hydrogen atoms which are considered distinguishable. © 2001 Published by Elsevier Science B.V.

PACS: 82.40.Dm; 34.50.Rk; 34.50.Lf

1. Introduction

The coherent control (CC) approach for controlling dynamical processes [1–24] makes use of quantum interference effects to manipulate the wave-like nature of matter. Specifically, CC utilizes coherent light sources to induce constructive or destructive interferences in the matter molecules. In this way one can enhance (or suppress) desired (or undesired) products. Numerous experimental demonstrations of the CC principle are now available [1–3].

Thus far, CC has been realized experimentally in the control of *unimolecular* processes, such as molecular photodissociation and photoionization [1–15]. Controlling the yield of *bimolecular reactions* [16–24] presents a much greater experimental challenge, since, as explained below, in this case one starts with an initially unbound state.

In recent years we have developed a number of scenarios by which bimolecular control could be achieved. Initially we investigated bimolecular laser control at energies below or near the reaction threshold [16–19]. Later, we presented a general theory for the control of bimolecular collisions, capable of dealing with energies above the reaction threshold [20]. This general theory has been applied to the control of isotopic variants of the $H + H_2 \rightarrow H_2 + H$ reaction [21] in the collinear domain. We have also studied the control of differential cross-sections of these reactions. Because

* Corresponding author. Fax: +1-416-978-5325.

E-mail address: pbrumer@tikva.chem.utoronto.ca (P. Brumer).

[1] Permanent address: Department of Chemical Physics, The Weizmann Institute of Science, 76100 Rehovot, Israel.

0301-0104/01/$ - see front matter
PII: S0301-0104(01)00256-7

of kinematic constraints [22], to be discussed below, we utilized, in both cases, superpositions of nearly degenerate diatomic states [23,24].

In the present paper we consider a more ambitious control scenario, involving fully realistic computations on superpositions of non-degenerate target-diatomic states. The experimental difficulty inherent in utilizing such target states as a basis for a superposition of scattering states, requiring correlating the translational energy of the atom with the internal energy of the target-diatomic molecule, is offset by the extensive degree of control afforded in this scheme. Below we demonstrate, with exact 3D quantum-mechanical calculations for isotopic variants of the $H + H_2 \rightarrow H_2 + H$ reaction using realistic potential energy surface, that total reactive vs non-reactive cross-sections can be extensively controlled by varying the phases and amplitudes of the initially prepared superposition state.

This paper is organized as follows: The preparation of the superposition of scattering state is discussed in Section 2.1. In Section 2.2 we summarize the implementation of CC for 3D atom–diatom quantum reactive scattering. The results of our calculations for $D + H_2$ and $H + H'D$ reactions (where H and H′ denote hydrogen atoms which are assumed to be distinguishable) are discussed in Section 3, where the wide range of control over reactive vs non-reactive cross-sections is demonstrated. Section 4 contains a brief summary.

2. Coherent control of atom–diatom reactive scattering

2.1. Initial preparation of a superposition of scattering state

Consider an atom A colliding with a diatomic molecule BC. The three possible outcomes (arrangements) of this collision are A + BC, B + AC, C + AB and we label each arrangement by the symbol $\alpha = a(A + BC)$, $b(B + AC)$, or $c(C + AB)$. Denoting the masses of the three atoms as M_A, M_B, M_C, and their positions as $\mathbf{r}_A$, $\mathbf{r}_B$, $\mathbf{r}_C$, we define $\mathbf{r}_{BC}$, the position of one target atom relative to the other, $\mathbf{K}$, the total center-of-mass wave vector, and $\mathbf{R}$, the total center-of-mass position, as,

$$\begin{aligned}
&M_{BC} = M_B + M_C, \quad M = M_A + M_{BC},\\
&\mu_{BC} = M_B M_C/(M_B + M_C),\\
&\mathbf{R}_{BC} = (M_B\mathbf{r}_B + M_C\mathbf{r}_C)/M_{BC},\\
&\mathbf{R} = (M_A\mathbf{r}_A + M_B\mathbf{r}_B + M_C\mathbf{r}_C)/M,\\
&\mathbf{r}_{BC} = \mathbf{r}_B - \mathbf{r}_C, \quad \mathbf{k}_{BC} = \mathbf{k}_B + \mathbf{k}_C,\\
&\mathbf{K} = \mathbf{k}_A + \mathbf{k}_{BC}.
\end{aligned} \tag{1}$$

We also define the arrangement-specific relative atom–diatom wave vector $\mathbf{k}$, and the relative atom–diatom position $\mathbf{r}$ for arrangement a as

$$\mathbf{k} = (M_{BC}\mathbf{k}_A - M_A\mathbf{k}_{BC})/M, \quad \mathbf{r} = \mathbf{r}_A - \mathbf{R}_{BC}. \tag{2}$$

Similar definitions hold for the two other (b and c) arrangements.

The total Hamiltonian of the system can be divided into four parts,

$$H = T(\mathbf{R}) + T(\mathbf{r}) + h_a(\mathbf{r}_{BC}) + V_a(\mathbf{r}, \mathbf{r}_{BC}), \tag{3}$$

where T denotes a kinetic-energy operator, h_a is the Hamiltonian for the BC diatomic and V_a is the atom–diatom interaction potential in the a arrangement, satisfying the asymptotic condition,

$$V_a \overset{\mathbf{r}\rightarrow\infty}{\rightarrow} 0. \tag{4}$$

The breakup of the Hamiltonian can be carried out in (three) different ways, depending on the arrangement index, α.

As shown previously [20], in order to assume control we need to create a superposition of continuum states, denoted as $|E, a, \mathbf{c}; 0\rangle$, comprised of $|E, a, \mathbf{n}; 0\rangle$, the eigenstates of the asymptotic arrangement Hamiltonian H_a,

$$H_a \equiv T(\mathbf{r}) + h_a(\mathbf{r}_{BC}), \tag{5}$$

satisfying the eigenvalue relation,

$$[E - H_a]|E, a, \mathbf{n}; 0\rangle = 0, \tag{6}$$

with $\mathbf{n}$ denoting the quantum numbers (such as vibration or rotation) describing the internal energetic states of the a arrangement separated products.

Assuming that we can create a superposition of two such states, we choose the atomic and diatomic incident wave functions ψ_A and ψ_{BC} as,

$$|\psi_A\rangle = |\phi_A(g)\rangle\{c_1 \exp[i\mathbf{k}_A(1)\cdot\mathbf{r}_A] + c_2 \exp[i\mathbf{k}_A(2)\cdot\mathbf{r}_A]\}, \quad (7)$$

$$|\psi_{BC}\rangle = c_3|\phi_{BC}(3)\rangle \exp[i\mathbf{k}_{BC}(3)\cdot\mathbf{R}_{BC}] + c_4|\phi_{BC}(4)\rangle \exp[i\mathbf{k}_{BC}(4)\cdot\mathbf{R}_{BC}], \quad (8)$$

where $|\phi_A(g)\rangle$ is the ground electronic state of atom A and $|\varphi_{BC}(j)\rangle$ are internal diatomic states with energy $e_{BC}(j)$. The total incident wave function is then given as,

$$|E,a,\mathbf{c};0\rangle = |\psi_A\rangle|\psi_{BC}\rangle = \sum_{i=1}^{2}\sum_{j=3}^{4}|A\rangle_{ij}\exp(i\mathbf{k}_{ij}\cdot\mathbf{r})\exp(i\mathbf{K}_{ij}\cdot\mathbf{R}), \quad (9)$$

where $|A\rangle_{ij} = c_i c_j|\phi_A(g)\rangle|\phi_{BC}(j)\rangle$, $\mathbf{k}_{ij} = (M_{BC}\mathbf{k}_A(i) - M_A\mathbf{k}_{BC}(j))/M$, and $\mathbf{K}_{ij} = \mathbf{k}_A(i) + \mathbf{k}_{BC}(j)$ with $(i = 1,2; j = 3,4)$.

If each term in the wave function has a different center-of-mass wave vector $\mathbf{K}_{ij}$, then Eq. (9) is composed of four independent incident waves. Since the V_a potential depends solely on the relative coordinates, $\mathbf{r}$ and $\mathbf{r}_{BC}$, and not on $\mathbf{R}$, the center-of-mass momentum is conserved (which is why we are able to separate out the center-of-mass coordinate from the relative coordinates). As a result, as shown in Ref. [22], only those $|\mathbf{K}\rangle$ components of the incident superposition state having the same center-of-mass momentum can interfere with each other to affect the final cross-sections. The interference between components with different $\mathbf{K}_I$ values is quickly washed away during the collision. However, conditions can be set in such a way that interference, and hence control, may be achieved. In order to do that, we require the equality of the center-of-mass motion of at least two energetically degenerate components,

$$\mathbf{K}_{13} = \mathbf{K}_{24}, \qquad \hbar^2 k_{13}^2/2\mu + e_{BC}(3) = \hbar^2 k_{24}^2/2\mu + e_{BC}(4), \quad (10)$$

with $\mu = M_A M_{BC}/M$. Eq. (9) then becomes

$$|E,a,\mathbf{c};0\rangle = \{|A\rangle_{13}\exp(i\mathbf{k}_{13}\cdot\mathbf{r}) + |A\rangle_{24}\exp(i\mathbf{k}_{24}\cdot\mathbf{r})\}\exp(i\mathbf{K}_{13}\cdot\mathbf{R}) + |A\rangle_{23}\exp(i\mathbf{k}_{23}\cdot\mathbf{r})\exp(i\mathbf{K}_{23}\cdot\mathbf{R}) + |A\rangle_{14}\exp(i\mathbf{k}_{14}\cdot\mathbf{r})\exp(\mathbf{K}_{14}\cdot\mathbf{R}), \quad (11)$$

where the term in the first bracket, due to Eq. (10), is a linear superposition of two degenerate states.

The cross-section resulting from the initial state in Eq. (11) is comprised of the first two terms of Eq. (11), which can interfere with each other because they have the same center-of-mass momentum, and by the last two ("satellite") terms, which are non-interfering because they have different center-of-mass momenta.

As a particular realization of Eq. (10) we choose $\mathbf{K}_{13} = \mathbf{K}_{24} = 0$ and $\mathbf{K}_{23} = -\mathbf{K}_{14}$, which means that $\mathbf{k}_A(1) = -\mathbf{k}_{BC}(3)$ and $\mathbf{k}_A(2) = -\mathbf{k}_{BC}(4)$. Since in that case $\mathbf{k}_{13} = \mathbf{k}_A(1)$, $\mathbf{k}_{24} = \mathbf{k}_A(2)$, we have from Eq. (10) that,

$$\hbar^2[k_A^2(1) - k_A^2(2)] = (2M_A M_{BC})[e_{BC}(4) - e_{BC}(3)]/(M_{BC} + M_A). \quad (12)$$

We also have in that case that, $\mathbf{k}_{23} + \mathbf{k}_{14} = \mathbf{k}_{13} + \mathbf{k}_{24} = \mathbf{k}_A(1) + \mathbf{k}_A(2)$, and assuming that $\mathbf{k}_A(1)$ is parallel to $\mathbf{k}_A(2)$, the energies of the satellite terms become,

$$E_{23}^{sat} = \frac{\hbar^2}{2\mu}k_{23}^2 + e_{BC}(3), \qquad E_{14}^{sat} = \frac{\hbar^2}{2\mu}k_{14}^2 + e_{BC}(4), \quad (13)$$

where

$$k_{23}^2 = \left[M_{BC}^2 k_A^2(2) + M_A^2 k_A^2(1) + 2M_A M_{BC} k_A(1)k_A(2)\right]/M^2,$$

$$k_{14}^2 = \left[M_{BC}^2 k_A^2(1) + M_A^2 k_A^2(2) + 2M_A M_{BC} k_A(1)k_A(2)\right]/M^2.$$

Note that in the specific case where we superpose degenerate states of the BC, Eq. (12) becomes $k_A^2(1) = k_A^2(2)$. Indeed, in this case we can choose $\mathbf{k}_A(1) = \mathbf{k}_A(2) = -\mathbf{k}_{BC}(3) = -\mathbf{k}_{BC}(4)$ so that all of the $\mathbf{K}_{ij}$ are equal and at the same time all of the four terms in Eq. (9) are energetically degenerate. Therefore, in the case corresponding to the scattering of an atom off a diatom in a superposition

of degenerate diatomic states, there are no extraneous uncontrollable satellite contributions. Results for this class of coherent control obtained for $D + H_2$, $H + D_2$ and $H + H'D$ reactions have been discussed in Refs. [22–24]. In this paper we consider another class of control, that utilizing superpositions of non-degenerate internal diatomic states.

2.2. Atom–diatom scattering using non-degenerate initial superposition states

Consider a superposition state involving non-degenerate diatomic states, given as,

$$|E,a,\mathbf{c};0\rangle = \sum_{i=1,2} c_i |\varphi_{\mathrm{A}}(g)\rangle |\varphi_{\mathrm{BC}}(v_i j_i m_i)\rangle |E_a^{\mathrm{kin}}(i)\rangle, \tag{14}$$

where, as above, c_i are complex coefficients. $|E_a^{\mathrm{kin}}(i)\rangle$ are plane waves describing the free motion of the A atom relative to the BC diatomic, whose energies are correlated to the energy levels of BC according to,

$$E_a^{\mathrm{kin}}(i) = E - e_{\mathrm{BC}}(v_i, j_i). \tag{15}$$

In this way all the components which make up the superposition state have the same total energy E.

With m_i quantum numbers taken to be helicities [25–27], i.e., the projections of $\mathbf{j}_i$ on $\mathbf{r}$, the relative atom–diatom (center-of-mass) position vector, the differential cross-section for forming the α-arrangement at scattering angles θ and φ, having started from the $|E,a,\mathbf{c};0\rangle$ superposition state, is given by

$$\sigma_{\alpha v j m \leftarrow a,\mathbf{c}}(E|\theta,\varphi) = \left| \sum_{i=1,2} c_i f_{\alpha v j m \leftarrow a v_i j_i m_i}(\pi-\theta,\varphi) \right|^2, \tag{16}$$

where

$$f_{\alpha v j m \leftarrow a v_i j_i m_i}(\theta,\varphi) = \frac{\mathrm{i}^{j_i - j + 1}\, \mathrm{e}^{\mathrm{i} m_i \varphi}}{2k_{a,v_i j_i}} \sum_J (2J+1) \times d^J_{m m_i}(\theta) T^J_{\alpha v j m \leftarrow a v_i j_i m_i} \tag{17}$$

is the scattering amplitude [27], $T^J_{\alpha v j m \leftarrow a v_i j_i m_i} = S^J_{\alpha v j m \leftarrow a v_i j_i m_i} - \delta_{\alpha a}\delta_{v v_i}\delta_{j j_i}\delta_{m m_i}$, $S^J_{\alpha v j m \leftarrow a v_i j_i m_i}$ are the elements of scattering S matrix in the helicity representation. Here J is the total angular momentum, m is the helicity of the product diatom, $d^J_{m m_i}(\theta)$ are the reduced rotation matrices [26,28], and $k_{a,v_i j_i} = (2\mu_a(E - e_{\mathrm{BC}}(v_i, j_i)))^{1/2}/\hbar$, with μ_a being the atom–diatom reduced mass in the a arrangement. The use of $\pi - \theta$, rather than θ, on the right-hand side of Eq. (16) is discussed in Ref. [29].

Explicitly squaring the sum in Eq. (16) (and dropping the initial state labels for convenience) and constructing the differential cross-section

$$\sigma^{\mathrm{R}}_{v j m}(\theta) = \int_0^{2\pi} \sigma^{\mathrm{R}}_{v j m}(\theta,\varphi)\,\mathrm{d}\varphi, \tag{18}$$

gives

$$\sigma^{\mathrm{R}}_{v j m}(\theta) = |c_1|^2 \sigma^{\mathrm{R}}_{v j m}(11|\theta) + |c_2|^2 \sigma^{\mathrm{R}}_{v j m}(22|\theta) + 2\,\mathrm{Re}\left\{ c_1 c_2^* \sigma^{\mathrm{R}}_{v j m}(12|\theta) \right\}, \tag{19}$$

$$\sigma^{\mathrm{R}}_{v j m}(ii|\theta) = \frac{\pi}{2k^2_{a,v_i j_i}} \sum_{J,J'} (2J+1)(2J'+1) d^J_{m m_i}(\pi-\theta) \times d^{J'}_{m m_i}(\pi-\theta) \times S^J_{\alpha v j m \leftarrow a v_i j_i m_i} \left[S^{J'}_{\alpha v j m \leftarrow a v_i j_i m_i} \right]^*, \quad a \neq \alpha, \quad i = 1,2, \tag{20}$$

and

$$\sigma^{\mathrm{R}}_{v j m}(12|\theta) = \frac{\pi i^{j_1 - j_2}}{2k_{a,v_1 j_1} k_{a,v_2 j_2}} \sum_{J,J'} (2J+1)(2J'+1) \times d^J_{m m_1}(\pi-\theta) d^{J'}_{m m_2}(\pi-\theta) S^J_{\alpha v j m \leftarrow a v_1 j_1 m_1} \times \left[S^{J'}_{\alpha v j m \leftarrow a v_2 j_2 m_2} \right]^* \delta_{m_1,m_2}, \quad a \neq \alpha. \tag{21}$$

Here we have taken into account that

$$\int_0^{2\pi} \mathrm{d}\varphi\, \mathrm{e}^{\mathrm{i}(m_1 - m_2)\varphi} = 2\pi \delta_{m_1,m_2}, \tag{22}$$

so that the interference term $\sigma^{\mathrm{R}}_{v j m}(12|\theta)$ is non-zero only when $m_1 = m_2$ and control therefore disappears for $m_1 \neq m_2$. Below, all superposition states used adhere to the $m_1 = m_2$ requirement. Note that above, the superscript R denotes reactive scattering into a specific final arrangement channel $\alpha \neq a$.

The total differential cross-section, $\sigma^{\mathrm{R}}(\theta)$, for reaction out of a state $|E,a,\mathbf{c};0\rangle$ is given as a sum over final states of the state-specific cross-sections,

$$\sigma^{\mathrm{R}}(\theta) = \sum_{v,j,m} \sigma^{\mathrm{R}}_{vjm}(\theta). \tag{23}$$

Integration of Eq. (19) over angle $\theta \in [0,\pi]$ gives the state-resolved integral reactive cross-section $\sigma^{\mathrm{R}}_{vjm}$. This can also be written as three terms, as in Eq. (19), but with $\sigma^{\mathrm{R}}_{vjm}(ij|\theta)$ replaced by $\sigma^{\mathrm{R}}_{vjm}(ij)$, where

$$\sigma^{\mathrm{R}}_{vjm}(ii) = \frac{\pi}{k^2_{a,v_i j_i}} \sum_J (2J+1) \left| S^J_{\alpha v j m \leftarrow a v_i j_i m_i} \right|^2, \quad i = 1,2, \tag{24}$$

$$\sigma^{\mathrm{R}}_{vjm}(12) = \frac{\pi i^{j_1 - j_2}}{k_{a,v_1 j_1} k_{a,v_2 j_2}} \sum_J (2J+1) S^J_{\alpha v j m \leftarrow a v_1 j_1 m_1} \times \left[S^J_{\alpha v j m \leftarrow a v_2 j_2 m_2} \right]^* \delta_{m_1,m_2}, \quad \alpha \neq a. \tag{25}$$

Averaged integral cross-sections are obtained by averaging over initial states and summing over the final states (we assume that $\Delta j = j_2 - j_1 > 0$)

$$\sigma^{\mathrm{R}}_{vj} = \frac{1}{2j_1+1} \sum_m \sum_{m_1} \left[|c_1|^2 \sigma^{\mathrm{R}}_{vjm}(11) + |c_2|^2 \sigma^{\mathrm{R}}_{vjm}(22) + 2\ \mathrm{Re}\left\{ c_1^* c_2 \sigma^{\mathrm{R}}_{vjm}(12) \right\} \right]. \tag{26}$$

Summing over the final states at energy E, we obtain the total integral cross-section as

$$\sigma^{\mathrm{R}} = \sum_{v,j} \sigma^{\mathrm{R}}_{vj}. \tag{27}$$

Note that state-to-state cross-sections $\sigma^{\mathrm{R}}_{vjm}(ii|\theta)$ and $\sigma^{\mathrm{R}}_{vjm}(ii)$ in Eqs. (20) and (24), as well as the corresponding total cross-sections $\sigma^{\mathrm{R}}(ii|\theta)$ and $\sigma^{\mathrm{R}}(ii)$, are the differential and integral cross-sections that appear in standard scattering theory (see, e.g., Ref. [25]), while $\sigma^{\mathrm{R}}_{vjm}(12|\theta)$ and $\sigma^{\mathrm{R}}_{vjm}(12)$ in Eqs. (22) and (25) and corresponding total cross-sections $\sigma^{\mathrm{R}}(12|\theta)$ and $\sigma^{\mathrm{R}}(12)$, are new types of interference terms which allow for control by varying the c_i coefficients. It is important to mention that significant control requires substantial $\sigma^{\mathrm{R}}(12)$ which follows from the Schwartz inequality $[|\sigma^{\mathrm{R}}(12)| \leqslant (\sigma^{\mathrm{R}}(11)\sigma^{\mathrm{R}}(22))^{1/2}]$, i.e., large $\sigma^{\mathrm{R}}(12)$ requires also large $\sigma^{\mathrm{R}}(11)$ and large $\sigma^{\mathrm{R}}(22)$. Therefore, extensive control is not limited to regions near the reactive threshold [16–19].

We can rewrite the total reactive cross-section in the more convenient form

$$\sigma^{\mathrm{R}} = [\sigma^{\mathrm{R}}(11) + x^2 \sigma^{\mathrm{R}}(22) + 2x|\sigma^{\mathrm{R}}(12)| \cos(\delta^R(12) + \phi_{12})]/(1+x^2), \tag{28}$$

where $x = |c_2/c_1|$, $\phi_{12} = \arg(c_2/c_1)$, and $\delta^{\mathrm{R}}(12) = \arg(\sigma^{\mathrm{R}}(12))$. Eq. (28) has the familiar form (see, e.g., Ref. [1]) which depicts the essence of CC. Specifically, there are two terms, $\sigma^{\mathrm{R}}(11)$ and $\sigma^{\mathrm{R}}(22)$, which result from independent routes to the product, plus an interference term, which is proportional to the complex term $\sigma^{\mathrm{R}}(12)$. The last term results from the simultaneous contributions of the two pathways.

In many cases, controlling the branching ratio between the reactive and non-reactive total cross-sections is of greatest interest. This ratio is given as,

$$\frac{\sigma^{\mathrm{R}}}{\sigma^{\mathrm{NR}}} = \frac{\sigma^{\mathrm{R}}(11) + x^2 \sigma^{\mathrm{R}}(22) + 2x|\sigma^{\mathrm{R}}(12)| \cos\left(\delta^{\mathrm{R}}(12) + \phi_{12}\right)}{\sigma^{\mathrm{NR}}(11) + x^2 \sigma^{\mathrm{NR}}(22) + 2x|\sigma^{\mathrm{NR}}(12)| \cos\left(\delta^{\mathrm{NR}}(12) + \phi_{12}\right)}. \tag{29}$$

In Eq. (29) the NR symbol denotes the non-reactive terms. These terms are analogous to the reactive terms except that α is replaced by a and T matrix elements replace the S matrix elements. A formula similar to Eq. (29) holds for the ratio of reactive to non-reactive differential cross-sections with $\sigma^{\mathrm{R}}(mn)$ replaced by $\sigma^{\mathrm{R}}(mn|\theta)$, etc.

It follows from Eqs. (28) and (29) that by varying the relative magnitude, x, and the relative phase, ϕ_{12} of the c_i coefficients, we can directly alter the interference term $\sigma(12)^{\mathrm{R}}$ (and/or $\sigma^{\mathrm{NR}}(12)$) and hence control the scattering cross-sections. The above approach can be readily extended to the case of a superposition of $N > 2$ interfering states.

3. Results and discussion

3.1. Computational details

We have applied this formulation to control the isotopic variants of the $H + H_2$ reaction: $D + H_2 \rightarrow DH + H$ and $H + H'D \rightarrow HH' + D$; $HD + H'$, where H and H′ are considered distinguishable. In our three-dimensional quantum-mechanical calculations, the $A + B_2$ symmetry [29] has been exploited for the first reaction for which there are only two final outcomes. We have restricted attention to initial superpositions made up of even H_2 rotational states (and assorted vibrational levels), i.e., only the even parity manifold for each partial wave was considered. In the second reaction, no such symmetry was assumed and three final arrangements were considered. The LSTH [30–32] potential energy surface was used in all calculations and the S matrices were obtained using a contracted-basis [33] log–derivative version of the Kohn variational principle [34].

The calculations in the $D + H_2$ reaction were carried out at two energies, $E = 0.93$ and 1.25 eV, for total angular momentum $J = 0, 1, \ldots, 31$ with $E_{\max} = 2.5$ eV and $j = 0, 2, 4, \ldots, 12$ and $j = 0, 2, 4, \ldots, 14$, respectively. The $H + H'D$ calculations were performed at total energy $E = 0.8$ eV for total angular momentum up to $J = 32$ with $j_{\max} = 14$ and $E_{\max} = 2.6$ eV. Here, $E_{\max}$ and $j_{\max}$ are respectively the maximum (cutoff) energy and maximum diatomic rotational quantum number of all diatomic basis states. The above sets of parameters ensure fully converged cross-sections for the chosen energies. The calculations reported here are CPU intensive, requiring in excess of 30 h of CRAY T90 time for each scattering computation.

3.2. Control of integral cross-sections

Of greatest practical interest is the ability to control integral cross-sections. We have explored the control of integral cross-sections of the $D + H_2 \rightarrow H + HD$ reaction at total energy $E = 1.25$ eV, which is well above the reaction threshold, thereby allowing us to demonstrate substantial control in the presence of a significant natural reactive cross-section.

Our numerical tests, carried out for various combinations of initial (v, j) states of H_2, show that control is substantial when superpositions of states with the same v quantum numbers are used. Initial superposition states with different v's do not lead to appreciable control. Hence, only equal-v results are reported here.

We first present results for scattering from an initial superposition state comprised of the $v_1 = 1$, $j_1 = 2$ and $v_2 = 1$, $j_2 = 4$ diatomic states (see Eq. (11)). Panel (a) of Fig. 1 presents a contour plot of σ^R/σ^{NR} ratio with contributions from the satellite terms ignored. The branching ratios are plotted as a function of the ϕ_{12} and $s = x^2/(1 + x^2)$ control parameters. (Note added in proof: a programming error requires that one change the ϕ_{12} to $-\phi_{12}$ in all figures in which it appears, in this paper as well as in Refs. [22,23].) Varying s from 0 to 1 corresponds to changing the initial superposition from being composed (at $s = 0$) of state 1 only, to being composed (at $s = 1$) of state 2 only .

The results clearly show substantial control over σ^R/σ^{NR}. This ratio can be increased by a factor of 2.5, from 0.14 for $s = 0.72$, $\phi_{12} = 131°$, to 0.35 for $s = 0.23$, $\phi_{12} = 308°$. These numbers should be compared with the "natural" branching ratios of 0.25 at $s = 0$ and 0.18 at $s = 1$.

Panel (b) of Fig. 1 shows the the σ^R/σ^{NR} ratio when the satellite terms are included. This has the effect of reducing slightly the range of control, which now only extends from 0.20 up to 0.33.

The range of control achievable gradually decreases with Δj of the rotational states which make up the superposition state. The origin of this behavior is evident from analysis of the results presented in Table 1 where the magnitude of both the reactive and non-reactive $\sigma(12)$ terms are seen to decrease sharply with increasing Δj. This leads, according to Eq. (29), to a decrease in the degree of control. The above behavior holds for both the $v_i = 0$ and $v_i = 1$ diatomic states.

In our computations the computational effort needed to evaluate the satellite terms of Eq. (11) at the two additional energies associated with the satellite terms was reduced by evaluating them at the same $E = 1.25$ eV energy of the main (interfering) term. The approximate σ^R/σ^{NR} ratios ob-

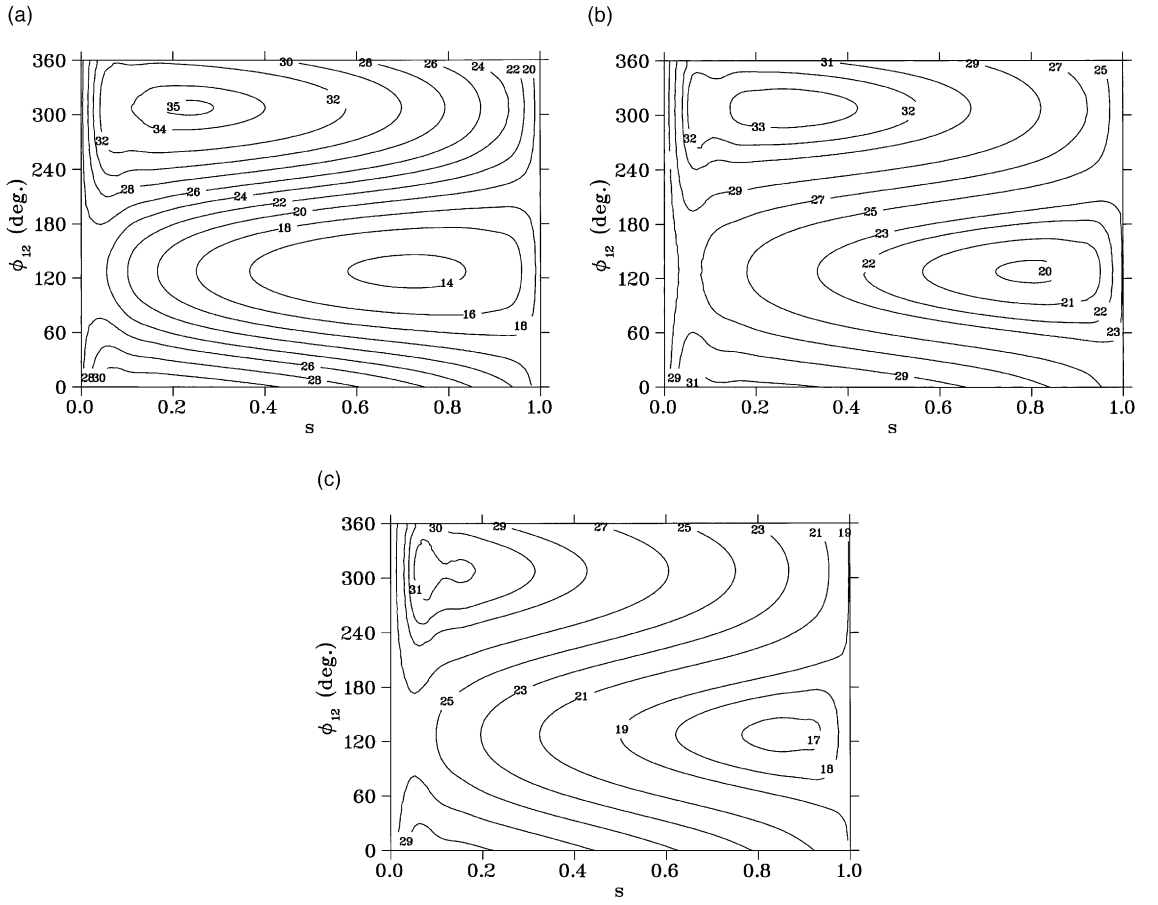

Fig. 1. Contour plot of the integral cross-sections ratio $\sigma^{R}/\sigma^{NR}(\times 10^2)$ for the $D + H_2$ reaction at total scattering energy $E = 1.25$ eV as a function of ϕ_{12} and s for a transition from an initial superposition state with $v_1 = 1$, $j_1 = 2$, $v_2 = 1$, $j_2 = 4$ calculated (a) without satellite terms, (b) with satellite terms obtained at energies given by Eq. (13) and (c) with satellite terms evaluated at energy $E = 1.25$ eV.

tained in this way, are in good agreement (compare panels (b) and (c) of Fig. 1) with the exact results. For example, the overall range of control is 72%, as compared to 65% in the more exact scheme. This favorable comparison has led us to use this approximation (which reduces the computational effort by a factor of 3) in all the calculations reported below.

Similar control results to those reported above are obtained for superposition states composed of $v = 0$ diatomic states. The best control has been obtained for scattering from the initial $(v_1 = 0, j_1 = 4, v_2 = 0, j_2 = 6)$ superposition state (see Table 1).

We now examine the range of control at $E = 0.93$ eV, an energy closer to the reaction threshold. Of the many cases studied, the most extensive control at that energy is obtained by choosing $(v_1 = 0, j_1 = 2, v_2 = 0, j_2 = 4)$ to build the initial superposition state. Fig. 2 shows the σ^{R}/σ^{NR} ratios for this case. By changing the phase angle ϕ_{12} from 93° at $s = 0.75$ to 269° at $s = 0.19$ we can vary σ^{R}/σ^{NR} from 0.16 to 0.29, as compared with the uncontrolled ratios of 0.24 at $s = 0$ and 0.18 at $s = 1$.

Control is also evident for scattering from the $(v_1 = 1, j_1 = 0; v_2 = 1, j_2 = 2)$ initial state, but in that case the ICS ratio is smaller by two orders of

Table 1
Integral cross-sections $\sigma^{NR,R}(mn)$ (in a_0^2), $m \leqslant n = 1, 2$, for $D + H_2$ collisions at $E = 1.25$ eV

v_1	j_1	v_2	j_2	$\sigma^{NR}(11)$	$\sigma^{NR}(22)$	$\sigma^{NR}(12)$	$\sigma^{R}(11)$	$\sigma^{R}(22)$	$\sigma^{R}(12)$
0	0	0	2	4.736(+1)	4.610(+1)	2.070(+0)	5.713(+0)	6.728(+0)	2.177(+0)
0	0	0	4	4.736(+1)	5.037(+1)	5.558(−1)	5.713(+0)	6.521(+0)	4.653(−1)
0	0	0	6	4.736(+1)	6.908(+1)	8.610(−3)	5.713(+0)	5.738(+0)	2.219(−1)
0	0	0	8	4.736(+1)	9.758(+1)	2.299(−1)	5.713(+0)	3.614(+0)	1.310(−1)
0	2	0	4	4.744(+1)	5.043(+1)	1.705(+0)	5.656(+0)	6.256(+0)	1.581(+0)
0	2	0	6	4.744(+1)	6.892(+1)	3.295(−1)	5.656(+0)	5.583(+0)	4.197(−1)
0	2	0	8	4.744(+1)	9.765(+1)	1.792(−1)	5.656(+0)	3.513(+0)	1.511(−1)
0	4	0	6	5.098(+1)	6.838(+1)	1.492(+0)	5.258(+0)	5.182(+0)	1.521(+0)
0	4	0	8	5.098(+1)	9.782(+1)	3.394(−1)	5.258(+0)	3.229(+0)	3.391(−1)
0	6	0	8	6.696(+1)	9.813(+1)	1.409(+0)	4.284(+0)	2.759(+0)	1.370(+0)
1	0	1	2	1.109(+2)	1.217(+2)	3.697(+0)	7.594(+0)	7.098(+0)	3.445(+0)
1	0	1	4	1.109(+2)	1.419(+2)	1.081(+0)	7.594(+0)	4.447(+0)	1.010(+0)
1	0	1	6	1.109(+2)	1.647(+2)	2.047(+0)	7.594(+0)	4.472(−1)	2.257(−1)
1	2	1	4	1.231(+2)	1.423(+2)	2.321(+0)	6.166(+0)	4.250(+0)	2.371(+0)
1	2	1	6	1.231(+2)	1.644(+2)	1.362(−1)	6.166(+0)	3.989(−1)	1.253(−1)
1	4	1	6	1.440(+2)	1.638(+2)	6.420(−1)	2.993(+0)	3.105(−1)	5.752(−1)

Quantum numbers v_i and j_i are explained in the text. The numbers in parentheses denote powers of 10.

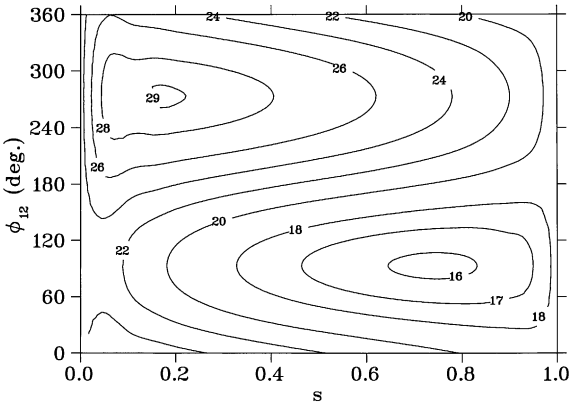

Fig. 2. The same as in Fig. 1 for scattering from an initial superposition state with $v_1 = 0$, $j_1 = 2$, $v_2 = 0$, $j_2 = 4$ at scattering energy $E = 0.93$ eV, including contributions from the uncontrolled satellite terms.

magnitude compared to the $v_i = 0$ case, due to the fact that at this energy the reactive cross-sections for $v_i = 1$ are much smaller than the non-reactive ones. The range of control quickly diminishes when higher values of j_i are involved or when $\Delta j > 2$. This can be understood by looking at Table 2 where the interference terms $\sigma(12)$ for $v_1 = v_2 = 1$ are tabulated and are seen to be much smaller than the diagonal $\sigma(nn)$ terms.

Consider next the $H + H'D$ reactions, calculated at total scattering energy of $E = 0.8$ eV, where H and H′ denote hydrogen atoms which are assumed distinguishable. In this case, we have two final reactive arrangement channels, $H' + HD(\alpha = b)$ and $D + HH'(\alpha = c)$. Our calculations show that control here is also attained mainly by choosing $\Delta v = 0$ and $\Delta j = 1$, 2. By contrast, control is practically non-existent for $\Delta v > 0$, or $\Delta j > 5$ or for $j_i > 8$. This behavior is consistent with Table 3 where we present the contributions of the diagonal and off-diagonal $\sigma(mn)$. We see that the $\sigma^R(12)$ terms are similar in magnitude to the corresponding diagonal terms for $\Delta j = 1$ or 2. This results in very extensive control (see Fig. 3). With increasing Δj, σ_{12}^R decreases, resulting, according to Eq. (29), in a smaller degree of control.

Looking specifically at scattering into the $H' + HD(\alpha = b)$ arrangement channel, our computations show that control is largest for superposition states composed of $v_1 = 0$, $j_1 = 2$, and $v_2 = 0$, $j_2 = 3$. The same holds true for the $v_1 = 0$, $j_1 = 2$, and $v_2 = 0$, $j_2 = 4$ superposition. σ^R/σ^{NR} for these cases, excluding the satellite contributions, are shown in Fig. 3(a) and (b), respectively. These figures display a very large range of control: The reactive to non-reactive ratio is seen to vary

Table 2
Integral cross-sections $\sigma^{NR,R}(mn)$ (in a_0^2), $m \leqslant n = 1, 2$, for $D + H_2$ collisions at $E = 0.93$ eV

v_1	j_1	v_2	j_2	$\sigma^{NR}(11)$	$\sigma^{NR}(22)$	$\sigma^{NR}(12)$	$\sigma^{R}(11)$	$\sigma^{R}(22)$	$\sigma^{R}(12)$
0	0	0	2	6.231(+1)	7.178(+1)	2.855(+0)	3.855(+0)	4.648(+0)	2.807(+0)
0	0	0	4	6.231(+1)	9.487(+1)	5.105(−1)	3.855(+0)	3.323(+0)	5.092(−1)
0	0	0	6	6.231(+1)	1.269(+2)	2.106(−1)	3.855(+0)	7.584(−1)	1.904(−1)
0	0	0	8	6.231(+1)	1.603(+2)	1.810(−2)	3.855(+0)	7.412(−3)	1.689(−2)
0	2	0	4	7.225(+1)	9.529(+1)	1.714(+0)	3.315(+0)	2.934(+0)	1.716(+0)
0	2	0	6	7.225(+1)	1.275(+2)	1.447(−1)	3.315(+0)	6.807(−1)	1.627(−1)
0	2	0	8	7.225(+1)	1.602(+2)	1.413(−2)	3.315(+0)	6.756(−3)	1.442(−2)
0	4	0	6	9.659(+1)	1.289(+2)	6.379(−1)	1.971(+0)	5.180(−1)	6.860(−1)
0	4	0	8	9.659(+1)	1.599(+2)	3.021(−2)	1.971(+0)	5.474(−3)	3.210(−2)
0	6	0	8	1.312(+2)	1.595(+2)	1.969(−2)	3.700(−1)	4.176(−3)	2.948(−2)
1	0	1	2	1.612(+2)	1.689(+2)	1.795(+0)	1.846(−1)	8.315(−2)	1.220(−1)
1	0	1	4	1.612(+2)	1.966(+2)	1.488(−2)	1.846(−1)	2.421(−5)	1.623(−3)
1	2	1	4	1.668(+2)	1.948(+2)	1.055(−1)	2.420(−2)	2.008(−5)	4.341(−4)

Table 3
Integral cross-sections $\sigma^{NR,R}(mn)$ (in c_1^2), $m \leqslant n = 1, 2$, for $H + H'D$ collisions at $E = 0.8$ eV[a]

j_1	j_2	$\alpha = 1$			$\alpha = 2$			$\alpha = 3$		
		$\sigma^{NR}(11)$	$\sigma^{NR}(22)$	$\sigma^{NR}(12)$	$\sigma^{R}(11)$	$\sigma^{R}(22)$	$\sigma^{R}(12)$	$\sigma^{R}(11)$	$\sigma^{R}(22)$	$\sigma^{R}(12)$
0	1	1.29(+2)	1.29(+2)	4.75(−1)	9.08(−1)	1.72(+0)	1.23(+0)	7.74(−1)	1.57(+0)	1.09(+0)
0	2	1.29(+2)	1.30(+2)	1.29(+0)	9.08(−1)	1.39(+0)	4.48(−1)	7.74(−1)	1.36(+0)	9.06(−1)
0	3	1.29(+2)	1.32(+2)	7.00(−2)	9.08(−1)	1.01(+0)	4.75(−1)	7.74(−1)	1.08(+0)	5.07(−1)
0	4	1.29(+2)	1.35(+2)	3.10(−1)	9.08(−1)	6.80(−1)	1.31(−1)	7.74(−1)	9.43(−1)	1.77(−1)
0	5	1.29(+2)	1.39(+2)	4.56(−2)	9.08(−1)	3.14(−1)	4.19(−2)	7.74(−1)	6.93(−1)	1.14(−1)
0	6	1.29(+2)	1.41(+2)	2.23(−1)	9.08(−1)	8.77(−2)	4.25(−2)	7.74(−1)	3.89(−1)	1.09(−1)
0	7	1.29(+2)	1.48(+2)	5.32(−2)	9.08(−1)	1.30(−2)	1.81(−2)	7.74(−1)	1.58(−1)	6.27(−2)
1	2	1.30(+2)	1.30(+2)	6.24(−1)	8.76(−1)	1.18(+0)	9.35(−1)	7.60(−1)	1.09(+0)	8.44(−1)
1	3	1.30(+2)	1.32(+2)	1.11(+0)	8.76(−1)	1.04(+0)	7.00(−1)	7.60(−1)	1.11(+0)	6.75(−1)
1	4	1.30(+2)	1.35(+2)	4.47(−2)	8.76(−1)	6.61(−1)	3.81(−1)	7.60(−1)	9.10(−1)	3.95(−1)
1	5	1.30(+2)	1.39(+2)	3.44(−1)	8.76(−1)	2.95(−1)	1.50(−1)	7.60(−1)	6.45(−1)	1.69(−1)
1	6	1.30(+2)	1.43(+2)	4.50(−2)	8.76(−1)	8.27(−2)	4.42(−2)	7.60(−1)	3.69(−1)	7.83(−2)
1	7	1.30(+2)	1.48(+2)	7.82(−2)	8.76(−1)	1.24(−2)	1.14(−2)	7.60(−1)	1.52(−1)	4.71(−2)
2	3	1.31(+2)	1.33(+2)	5.95(−1)	7.80(−1)	8.04(−1)	7.33(−1)	7.15(−1)	8.48(−1)	7.16(−1)
2	4	1.31(+2)	1.35(+2)	9.55(−1)	7.80(−1)	5.67(−1)	5.07(−1)	7.15(−1)	7.88(−1)	5.41(−1)
2	5	1.31(+2)	1.39(+2)	5.18(−2)	7.80(−1)	2.62(−1)	2.59(−1)	7.15(−1)	5.82(−1)	3.07(−1)
2	6	1.31(+2)	1.43(+2)	2.22(−1)	7.80(−1)	7.44(−2)	9.53(−2)	7.15(−1)	3.37(−1)	1.34(−1)
2	7	1.31(+2)	1.48(+2)	3.71(−2)	7.80(−1)	1.14(−2)	2.34(−2)	7.15(−1)	1.41(−1)	5.47(−2)
3	4	1.33(+2)	1.36(+2)	3.70(−1)	5.90(−1)	4.39(−1)	4.78(−1)	6.22(−1)	6.16(−1)	5.70(−1)
3	5	1.33(+2)	1.39(+2)	7.99(−1)	5.90(−1)	2.15(−1)	2.85(−1)	6.22(−1)	4.87(−1)	3.98(−1)
3	6	1.33(+2)	1.43(+2)	8.53(−2)	5.90(−1)	6.33(−2)	1.22(−1)	6.22(−1)	2.95(−1)	2.09(−1)
3	7	1.33(+2)	1.48(+2)	1.17(−1)	5.90(−1)	9.94(−3)	3.47(−2)	6.22(−1)	1.26(−1)	8.53(−2)
4	5	1.36(+2)	1.39(+2)	1.21(−1)	3.44(−1)	1.72(−1)	2.31(−1)	4.84(−1)	3.94(−1)	4.03(−1)
4	6	1.36(+2)	1.43(+2)	6.45(−1)	3.44(−1)	5.22(−2)	1.11(−1)	4.84(−1)	2.48(−1)	2.52(−1)
4	7	1.36(+2)	1.48(+2)	9.07(−2)	3.44(−1)	8.46(−3)	3.54(−2)	4.84(−1)	1.10(−1)	1.17(−1)
5	6	1.40(+2)	1.43(+2)	5.71(−1)	1.41(−1)	4.32(−2)	7.46(−2)	3.24(−1)	2.07(−1)	2.39(−1)
5	7	1.40(+2)	1.48(+2)	4.22(−1)	1.41(−1)	7.14(−3)	2.64(−2)	3.24(−1)	9.40(−2)	1.28(−1)
6	7	1.43(+2)	1.48(+2)	1.01(+0)	3.66(−2)	6.08(−3)	1.42(−2)	1.75(−1)	8.05(−2)	1.10(−1)

[a] Cross-sections for $\alpha = 2$ and $\alpha = 3$ correspond to the $H' + HD$ and $D + H_2$ final arrangements, respectively. Results for scattering from initial states with $v_i = 0$ only are shown.

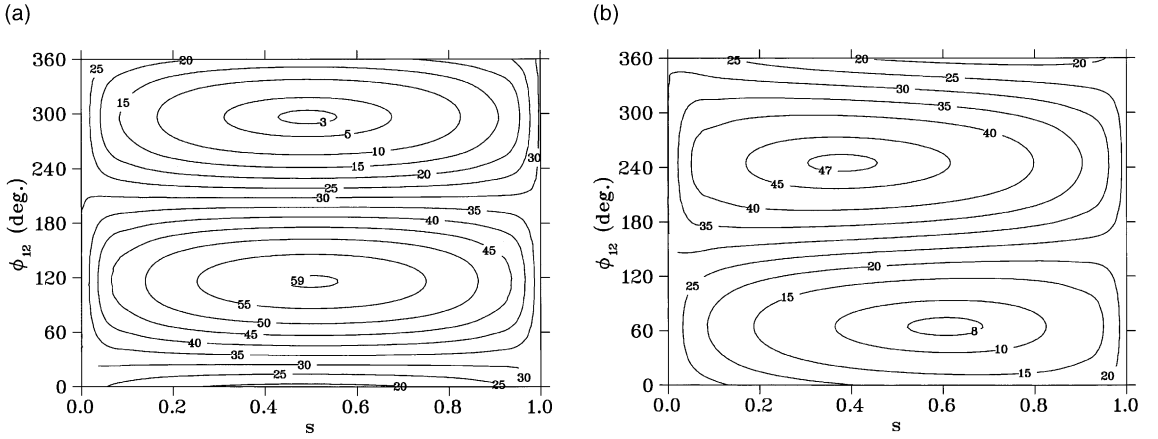

Fig. 3. Contour plot of the integral cross-sections ratio $\sigma^{R}/\sigma^{NR}(\times 10^3)$, obtained without accounting for satellite terms, for the $H + H'D$ reaction at total scattering energy $E = 0.8$ eV as a function of ϕ_{12} and s, for a transition to the $H' + HD$ final arrangement from an initial superposition state with (a) $v_1 = 0$, $j_1 = 2$, $v_2 = 0$, $j_2 = 3$, and (b) $v_1 = 0$, $j_1 = 2$, $v_2 = 0$, $j_2 = 4$.

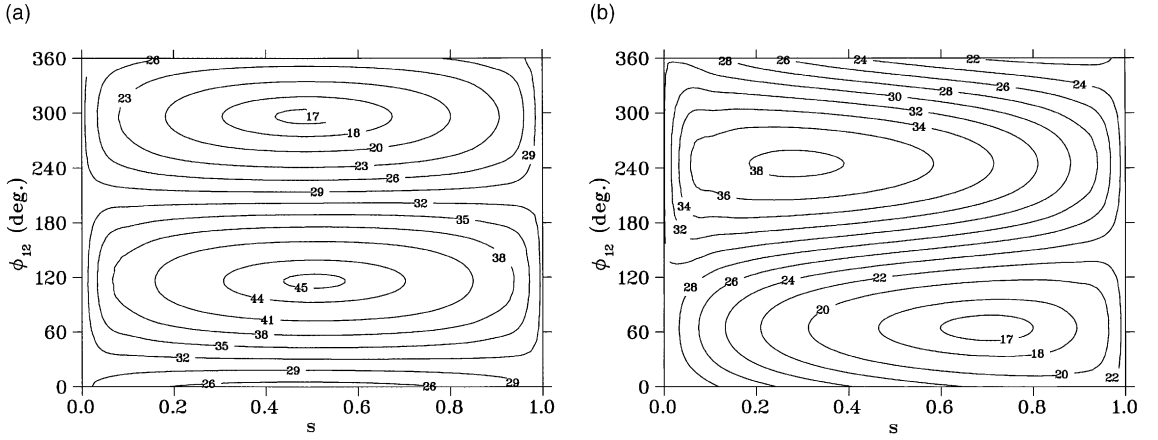

Fig. 4. The same as in Fig. 3 including the contribution from the uncontrolled satellite terms.

from 0.003 to 0.059 (a factor of 19.7) for the first case, and from 0.008 to 0.047 (a factor of 5.9) for the second case.

The results for the same superposition states obtained by taking into account the contributions from two uncontrolled satellite terms are presented in Fig. 4(a) and (b). Substantial control over σ^{R}/σ^{NR} ratio is clearly seen even in the presence of the satellite terms. One can also see that control is larger for the transition with $\Delta j = 1$ (see Fig. 4(a)). For example, by changing ϕ_{12} from 120° to 300° at $s = 0.51$, we can change σ^{R}/σ^{NR} for an initial superposition of the $v_1 = 0$, $j_1 = 2$, and $v_2 = 0$, $j_2 = 3$ states from 0.017 to 0.045, as compared with the "natural" ratio of 0.031.

Essentially the same level of control may be achieved by using a superposition of the $v_1 = 0$, $j_1 = 2$ and $v_2 = 0$, $j_2 = 4$ states (see Fig. 4(b)). In this case, the ICS ratio varies from 0.017 to 0.038. Here too we find that the range of control decreases with increasing Δj (see, e.g., Table 3), and that control is essentially non-existent for $\Delta v > 0$.

Finally, consider the $D + HH'$ $(\alpha = c)$ arrangement. In this case, the largest control is

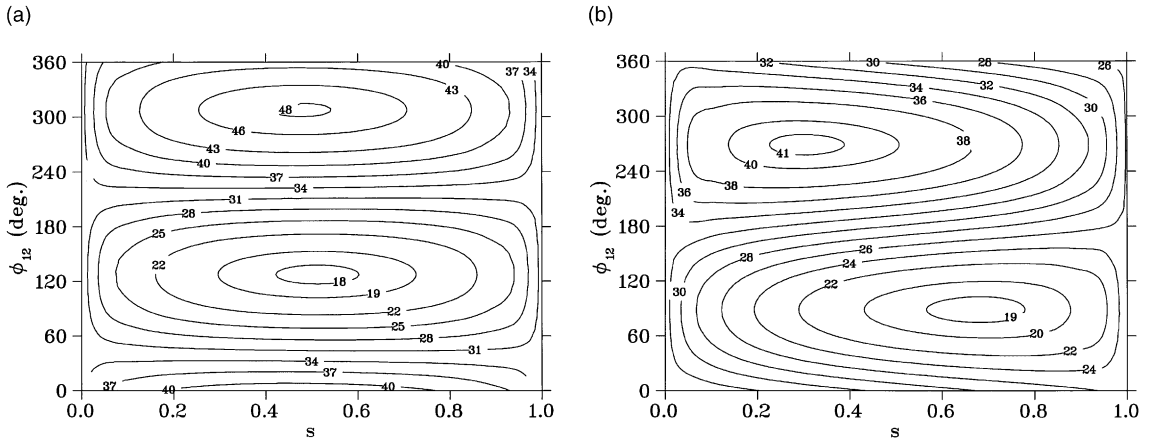

Fig. 5. Contour plot of the integral cross-sections ratio $\sigma^{R}/\sigma^{NR}(\times 10^3)$ (with uncontrolled satellite terms) for the $H + H'D$ reaction at total scattering energy $E = 0.8$ eV as a function of ϕ_{12} and s, for a transition to the $D + HH'$ final arrangement from an initial superposition state with (a) $v_1 = 0$, $j_1 = 3$, $v_2 = 0$, $j_2 = 4$, and (b) $v_1 = 0$, $j_1 = 3$, $v_2 = 0$, $j_2 = 5$.

achieved by scattering from a superposition of the $v_1 = 0$, $j_1 = 3$ and $v_2 = 0$, $j_2 = 4$ states or the $v_1 = 0$, $j_1 = 3$ and $v_2 = 0$, $j_2 = 5$ states. A substantial range of control over reactive to non-reactive branching ratios in these two cases is displayed in Fig. 5(a) and (b), respectively. As shown in Fig. 5(a), the ICS ratio can be made to change from 0.018 to 0.048, compared with the "natural" ratio of 0.033. The results for the second case are similar.

4. Summary

In this work, we have demonstrated that it is possible to substantially control the reactive to non-reactive integral branching ratios by using a superposition of non-degenerate continuum states. The demonstration was carried out for realistic 3D reactive scattering models of the $D + H_2 \rightarrow DH + H$ and the $H + H'D \rightarrow HH' + D$; $HD + H'$ reactions. Control is due to both a constructive enhancement of reactive cross-sections and a destructive depletion of the non-reactive ones, or vice versa.

Kinematic laboratory constraints pertaining to bimolecular control lead to uncontrolled satellite terms. Nevertheless, even in the presence of these uncontrolled terms, extensive control over total cross-sections has been demonstrated, making the laboratory confirmation of our present predictions a realistic possibility.

Acknowledgements

This work was supported in part by the US Office of Naval Research, Photonics Research Ontario and by a grant of HPC time on the CRAY T90 and SV1 from the DoD NAVOCEANO MSRC Center.

References

[1] M. Shapiro, P. Brumer, Trans. Far. Soc. 93 (1997) 1263.
[2] P. Brumer, M. Shapiro, Annu. Rev. Phys. Chem. 43 (1992) 257.
[3] A. Shnitman, I. Sofer, I. Golub, A. Yogev, M. Shapiro, Z. Chen, P. Brumer, Phys. Rev. Lett. 76 (1996) 2886.
[4] C. Asaro, M. Shapiro, P. Brumer, Phys. Rev. Lett. 60 (1988) 1634.
[5] M. Shapiro, J.W. Hepburn, P. Brumer, Chem. Phys. Lett. 149 (1988) 451.
[6] C. Chen, Y.-Y. Yin, D.S. Elliott, Phys. Rev. Lett. 64 (1990) 507.
[7] C. Chen, Y.-Y. Yin, D.S. Elliott, Phys. Rev. Lett. 65 (1990) 1737.
[8] S.M. Park, S.-P. Lu, R.J. Gordon, J. Chem. Phys. 94 (1991) 8622.
[9] B.A. Baranova, A.N. Chudinov, B.Ya. Zel'dovitch, Opt. Commun. 79 (1990) 116.

[10] V.D. Kleiman, L. Zhu, X. Li, R.G. Gordon, J. Chem. Phys. 102 (1995) 5863.
[11] B. Kohler, J.L. Krause, F. Raski, K.R. Wilson, V.V. Yakovlev, R.M. Whitnell, Y. Yan, Acct. Chem. Res. 28 (1995) 133.
[12] W.S. Warren, H. Rabitz, M. Dahleh, Science 259 (1993) 1581.
[13] S.A. Rice, Science 258 (1992) 412.
[14] B. Sheehy, B. Walker, L.F. DiMauro, Phys. Rev. Lett. 74 (1995) 4799.
[15] E. Dupont, P.B. Corkum, H.C. Liu, M. Buchanan, Z.R. Wasilewski, Phys. Rev. Lett. 74 (1995) 3596.
[16] M. Shapiro, Y. Zeiri, J. Chem. Phys. 85 (1986) 6449.
[17] T. Seideman, M. Shapiro, J. Chem. Phys. 88 (1988) 5525.
[18] T. Seideman, J.L. Krause, M. Shapiro, Faraday Disc. Chem. Soc. 91 (1991) 271.
[19] J.L. Krause, M. Shapiro, P. Brumer, J. Chem. Phys. 92 (1990) 1126.
[20] M. Shapiro, P. Brumer, Phys. Rev. Lett. 77 (1996) 2574.
[21] D. Holmes, M. Shapiro, P. Brumer, J. Chem. Phys. 105 (1996) 9162.
[22] A. Abrashkevich, M. Shapiro, P. Brumer, Faraday Discuss. 113 (1999) 291.
[23] A. Abrashkevich, M. Shapiro, P. Brumer, Phys. Rev. Lett. 81 (1998) 3789.
[24] A. Abrashkevich, M. Shapiro, P. Brumer, Phys. Rev. Lett. 82 (1999) 3002.
[25] J.R. Taylor, Scattering Theory, Wiley, New York, 1972.
[26] W.H. Miller, J. Chem. Phys. 50 (1969) 407.
[27] G.C. Schatz, A. Kuppermann, J. Chem. Phys. 65 (1976) 4642.
[28] R.T. Pack, G.A. Parker, J. Chem. Phys. 87 (1987) 3888.
[29] J.Z.H. Zhang, W.H. Miller, J. Chem. Phys. 91 (1989) 1528.
[30] P. Siegbahn, B. Liu, J. Chem. Phys. 68 (1978) 2457.
[31] D.G. Truhlar, C.J. Horowitz, J. Chem. Phys. 68 (1978) 2466.
[32] D.G. Truhlar, C.J. Horowitz, J. Chem. Phys. 71 (1979) 1514.
[33] D.E. Manolopoulos, M. D'Mello, R.E. Wyatt, J. Chem. Phys. 93 (1990) 403.
[34] D.E. Manolopoulos, R.E. Wyatt, Chem. Phys. Lett. 152 (1988) 23.